

Use of Vertical Electrical Sounding for Delineating Groundwater Contamination in the Uplands Wadi Rasyan, Taiz, Yemen.

Hamza A. Ibrahim, Ahmed. S. Al Gabery*
and Ahmed A. Abdulqader**

Geology Department, Assuit University, Egypt.

**Geology Department, Sana'a University, Yemen.*

***Geology Department, Taiz University, Yemen.*

*ibraibraibra@yahoo.com, Sufian97@hotmail.com &
drahaziz@yahoo.com*

Received: 13/10/2009

Accepted: 04/01/2011

Abstract. Fresh water is becoming increasingly scarce in Taiz city, Yemen, partly due to a growing population and in part due to pollution of near surface aquifers by municipal and industrial wastes. Electrical depth sounding has been found to be powerful tool to delineate subsurface contaminated zones. The measured apparent resistivity and 1D inversion models have been used to construct apparent maps and 2D geoelectrical cross-sections displaying the variation of resistivity of the subsurface layers.

In the present study, a vertical electrical sounding (VES) was conducted using the shlumberger array at 38 sites distributed over six profiles along the most important wadis in the Uplands Wadi Rasyan, Taiz, Yemen. The objectives of this study were: (1) to locate the distribution of contamination zones, and (2) to investigate the subsurface geology and the geologic structures that may affect the spreads of contamination zones.

It was revealed that the area is highly affected by the contamination from the sewage and industrial effluents which were observed as: Four shallow contamination zones concentrated around the contaminant sources in Wadi Al Hawban, Al Hawgala, Hidran, and along the main stream of Wadi Rasyan. They have various horizontal and vertical extensions, some reached to 15 Km long, 2 Km width and extend to about 30 m depth in the shallow alluvial aquifer

to greater than 150 m depth. The shape, size, and trends of these zones are restricted by faults, fractures and geologic contacts.

Introduction

Uplands Wadi Rasyan is the mountainous part of Wadi Rasyan that drains the southwestern Yemen Mountains into Tihama coastal plain. The area extends between the latitudes $13^{\circ} 23'$ and $13^{\circ} 53'$ North, and the longitudes $43^{\circ} 37'$ and $44^{\circ} 10'$ East (Fig.1). It covers about 1806 km^2 with a total population of about 1,200,000, including Taiz city with a total population of about 600,000.

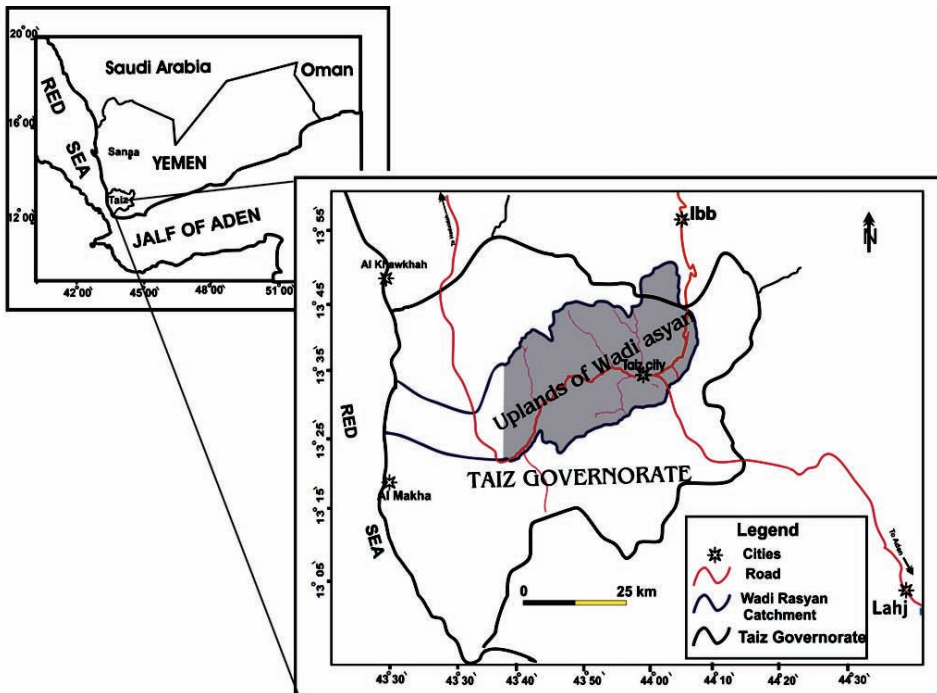


Fig. 1. Location map of the study area.

In the study area, the groundwater has deteriorated significantly with time due to continuous discharging of waste water and other pollutants from the city and industrial sites. The average total dissolved solids (TDS) in Hawgala and Hawban wells have increased from about 1000 mg/l in 1964 to about 2,400 mg/l in 1974 (JMM, 1974), and reached to about 3000 mg/l in 1996 (Welle, 1997). According to

Abdulgader (2005), the average TDS in the same areas was about 4000 mg/l in 2002. The mentioned problems in addition to the lack of comprehensive studies dealing with the contamination problems, have urged us to perform the present investigation.

Measured resistivity values are controlled by material resistivity, and the presence, quality, and quantity of ground water (Haeni and others, 1993). The resistivity of a fracture zone is controlled by the secondary porosity, and the presence of altered secondary minerals and/or precipitate. The maximum penetration depth is directly proportional to the electrode spacing and inversely proportional to the subsurface conductivity (Edwards, 1977). This property together with the low cost, make the direct current (DC) resistivity methods very suitable for groundwater exploration. So, it have been widely used for groundwater contamination detection (*e.g.* Cartwright and McComas, 1968; Warner, 1969; Stoller and Roux, 1973; Klefstad *et al.*, 1975; Barker, 1990; Carpenter *et al.*, 1990; Whiteley and Jewell, 1992; Meju, 1993; Powers, *et al.*, 1999; and Maxwell., 2000).

In the present study, direct current resistivity survey was carried out by using the Vertical Electrical Sounding (VES) technique and Schlumberger array to recognize the vertical and horizontal distribution of the contamination zones and to identify the structural effect on the shape and direction of contaminant spreads.

Geological Setting

The study area occupies the southwestern corner of Arabian shield. As shown in Fig. 2, the geology of the area is very complex due mainly to its location at the junction of the Red Sea and Gulf of Aden rift systems. Paleozoic sedimentary rocks outcrop in relatively small areas in the middle and northeast of the catchment. While, Tertiary volcanics are the dominant rock unit, made of sequences of basic and acidic lavas, fissure eruption and pyroclastics with sedimentary intercalations (Kruck, *et al.*, 1996), Miocene granite intruded in the south east of the area, loose Quaternary sediments and recent alluvial deposits cover Al Janad plateau and fill the wadis and plains. The structure of the area is very complicated also due to large number of faults, dykes and volcanic intrusions. The major faults are oriented N-S to NNW, NW and NE. Most of them are high angle normal faults. The majority of feeding

fissures and older plateau dikes are oriented parallel to the NW-SE direction (Calpайди, *et al.*, 1987a; and La Davison, *et al.*, 1994). The tectonic movements and the Red Sea rifting in addition to the granitic intrusions have created a series of horst and graben structures, the staircase-like structures with the general subsidence towards the west are predominant in the middle part. The main structural features in the study area are; Taiz graben, Al Barh half graben and large plutonic bodies of Jabal Sabir and Jabal Habashi granitic intrusions.

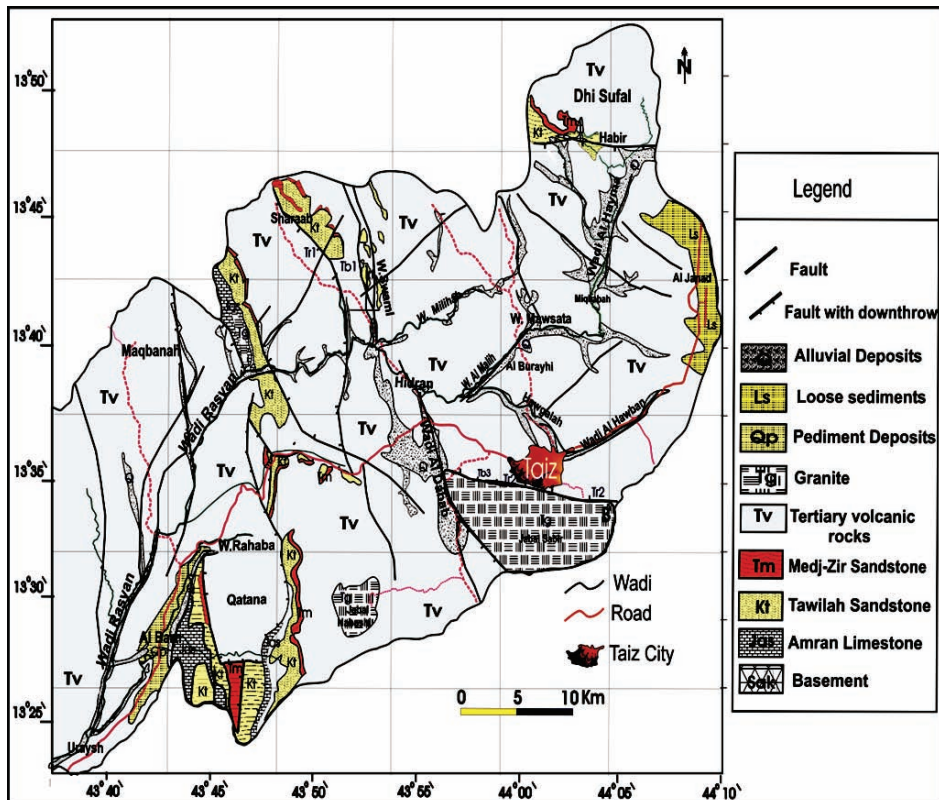


Fig. 2. Geological map of the Uplands of Wadi Rasyan, Taiz, Yemen, adopted after Kruck and Schäffer, 1991 and DEY, 1997.

Methodology

Field Survey and Data Acquisition

A total of 38 vertical electrical sounding sites were selected because of possibility for groundwater contamination. The VES-sites

were distributed along six profiles *A-A'*, *B-B'*, *C-C'*, *D-D'*, *E-E'* and *F-F'* (Fig.3). Some soundings were conducted at the site on or very close to existing boreholes for correlation purpose. Four sounding data (VES-es 35, 36, 37 and 38) were taken from DEY (1997) and reinterpreted to fill some gaps along profiles *A-A'*, and *B-B'*.

ABEM Terrameter SAS 1000 was used for the data acquisitions. The Schlumberger electrode configuration at the sounding sites was spread parallel to the previously known fault zones, and the maximum current electrode spacing ranged between 600 and 1400 m.

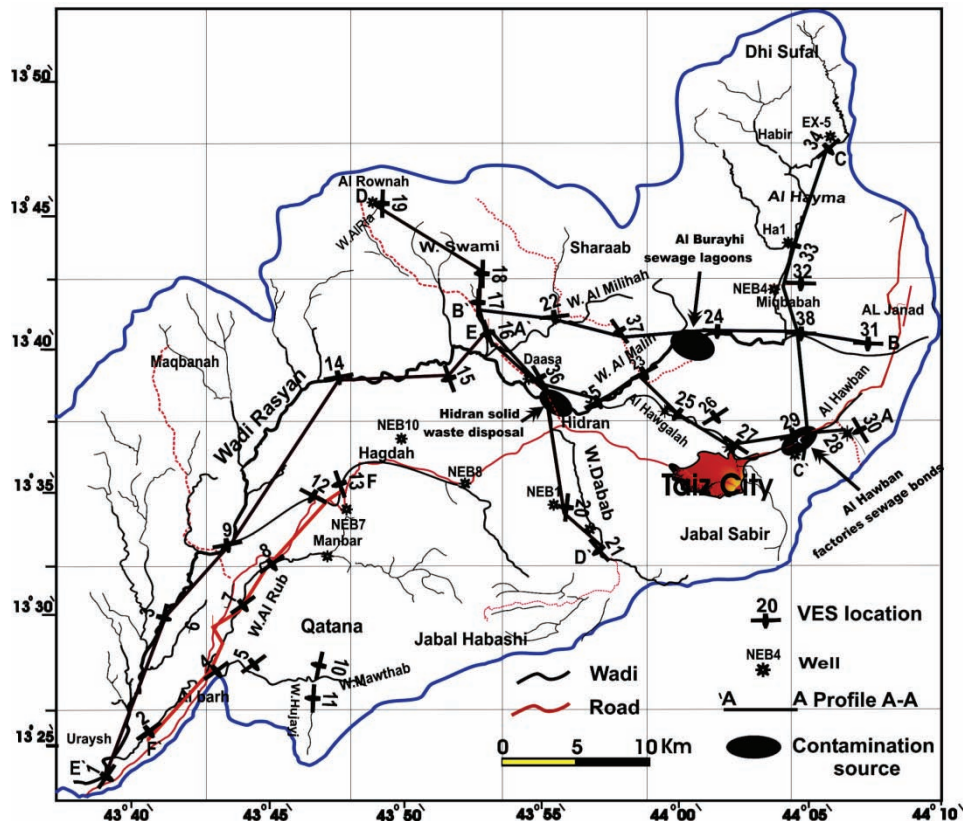


Fig. 3. Map showing the locations of VES-Stations, geoelectrical profiles, calibration wells, and locations of the contamination sources.

Geoelectrical Calibration Model

The specific resistivity R_b of layer containing water is expressed as: $R_b = F \cdot R_w$; where F is the formation factor, R_w is the resistivity of

water. The formation factor F depends on the porosity, sorting, clay content, and the degree of consolidation or cementation of the sediments. Compact and unfractured dry rocks may be characterized by a resistivity of up to 10,000 Ohm.m (Telford *et al.*, 1976). The electrical resistivity values of fractured/ alternated and unconsolidated rocks, depending on fluid-saturation, decrease to very low values. The resistivity of groundwater can vary over several orders of magnitude depending on its salinity. Fresh waters tend to be resistive while saline brines are very conductive (Telford *et al.*, 1976). The resistivity of a layer saturated by saline water and some dissolved solids is in the range of 8 to 50 Ohm.m (De Breuk and De Moor, 1969, Goodell, 1986, Flanzenbaum, 1986, and Zohdy *et al.*, 1993).

Based on the previously mentioned features, a modified geoelectrical model was developed (Table 1), and used as a guide for the interpretation of resistivity data in the present study. Accordingly, subsurface of the study area was subdivided into three primary geologic units as the following:

a) The first, shallow with resistivity range from 5 Ohm.m to greater than 400 Ohm.m and thickness between 10 to 50m, is correlated with the top alluvial deposits.

b) The second is a geoelectric unit of resistivity ranges from 5 to 60 Ohm.m and reached in thickness to about 400 m, is interpreted as fractured volcanic (fracture basalt, pyroclastics and tufficious breccias) containing mineralized water.

c) The third geoelectric unit has electrical resistivity ranges between 60 to greater than 200 Ohm.m; this layer is interpreted as hard volcanic (basalt, rhyolite, and granite). In some areas, this layer is represented as water bearing sandstone. While the deepest geoelectric layer is represented as bed rocks, Hard basalt, Rhyolite dyke complex, Limestone, or Precambrian basement) with resistivity (> 150 Ohm.m).

Each of the major units was divided into different zones according to the percentage of clay, degree for fracturing, water saturation and its salinity or degree of contamination.

Table 1. Calibration model of resistivity for the various layers in the study area (modified after DHV, 1986 and Abdulqader, 2005).

	Rock Type	Fluid content	Resistivity range (Ohm m)	Resistivity zone
Alluvial	Top soil	Dry	30-60	Intermediate
	Top Soil	Wet	15-24	Low
	Sand & Gravel	Dry	36->400	High
	Clay sand	Dry	11- 40	Low
	Silt-Sand & gravels	Fresh water	20- 65	Intermediate
	Silt-Sand & gravels	Contaminated water	<10	Very low
Fracture volcanic	Tuff and acidic volcanic	Brackish water	25 - 70	Intermediate
	Fracture basalt	Brackish water	10-45	Low
	Fracture basalt & breccias	Contaminated water	2-20	Very low
Bed rocks	Hard basalt & acidic volcanic	Dry	>160	High
	Weathered sandstone	Dry	> 80	High
	Saturated sandstone	Fresh water	60-100	High
	Compacted sandstone	Fresh water	80-110	High
	Limestone	-----	>130	Very high
	Basement & Dyke complex	-----	>400	Very high

Data Processing and Interpretation

The measured data from the resistivity survey are the apparent resistivities in a cross-section of the earth; they were processed through the following steps:

1. The field measurements were processed and interpreted using two software programs, RESIX-P (Interpex, 1993) and IPI2win (Geoscan-M, 2001). The results of these interpretations classified the investigated subsurface sequence into four to six successive geoelectric layers of different resistivity ranges, thickness, and depth. An example of the outputs from the inversion process by using RESIX-P and IPI2win programs is shown in Fig. 4. The inversion models (true resistivities ρ and thicknesses T) at each sounding station are listed on Table 2.
2. The accuracy of the results was confirmed through correlations with the geological and other geophysical data available at each location. The geological data obtained from the observation wells NEB1, NEB4, and EX-5 are used for comparison with the layered earth geoelectric

models (Fig. 5). The hydrochemical data (e.g. Welle, 1997; and Abdulqader, 2005) were used also to confirm the resistivity data. Of which, 12 water samples collected from the highly contaminated areas were listed in Tables 3 & 4.

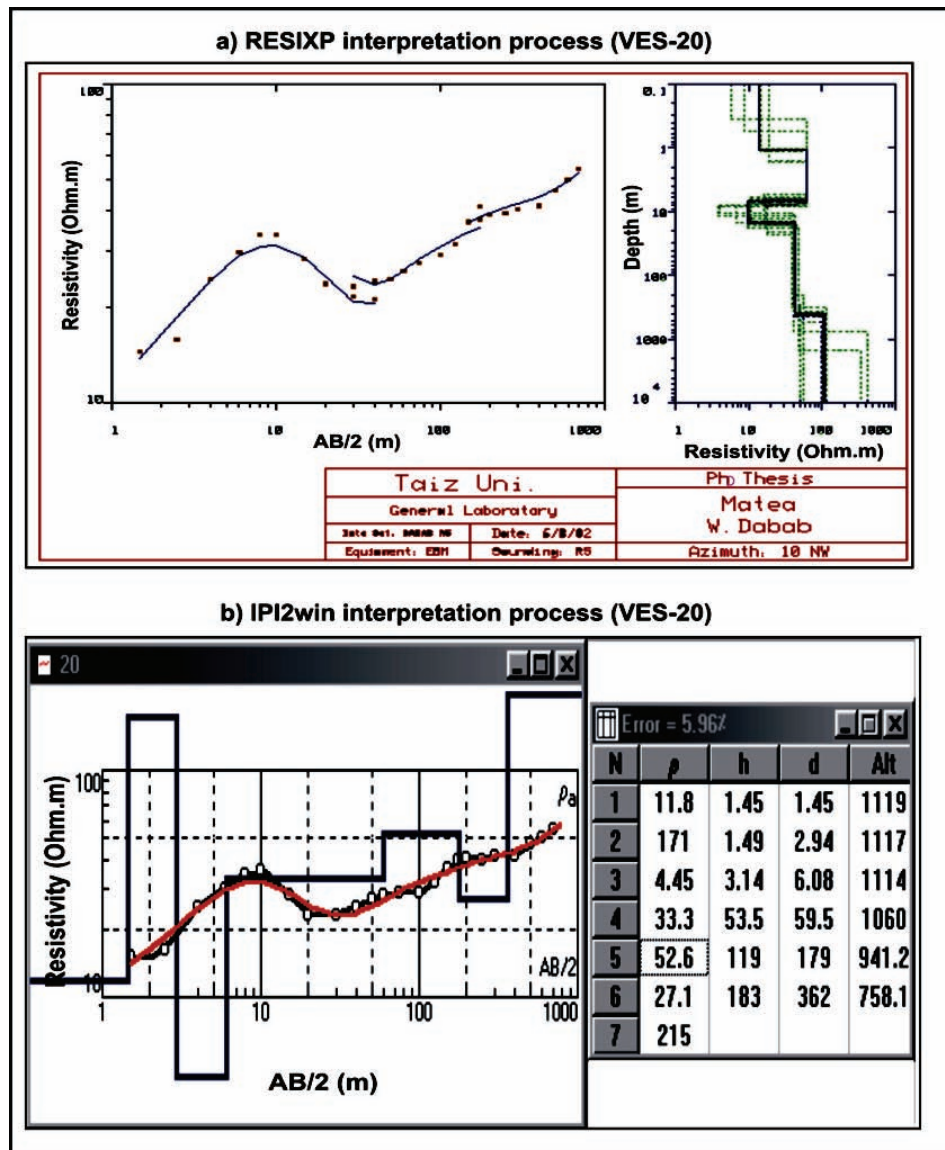


Fig. 4. An example of inversion output of RESIXP and IPI2win software.

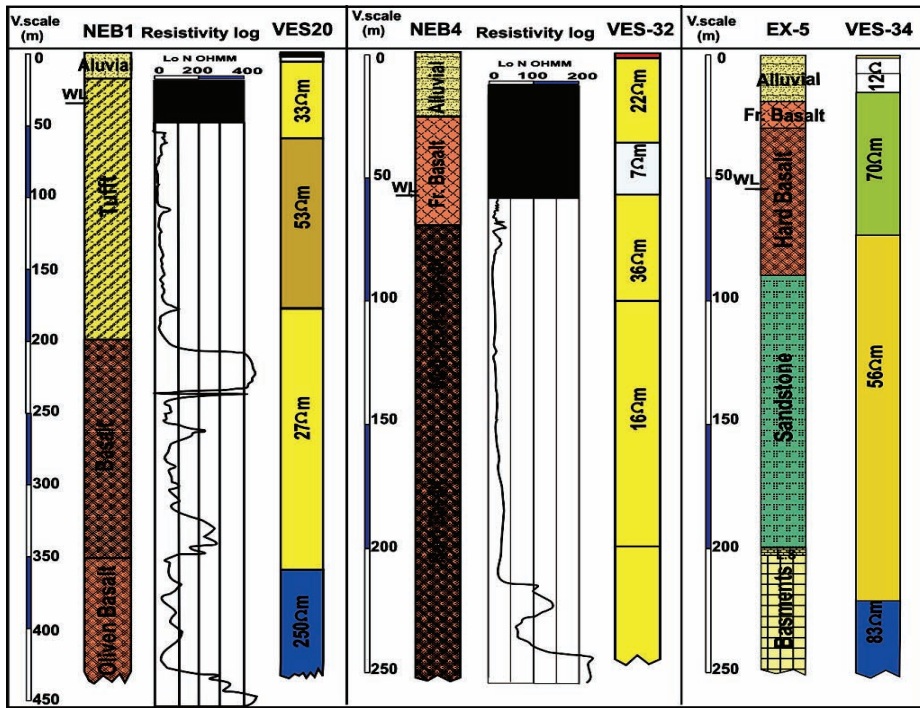


Fig. 5. An example of interpretative resistivity models correlated with lithological cross sections and resistivity logs of the nearby wells.

3. The field measuring data including VES-locations, electrodes distances AB/2, and the apparent resistivity values ρ_a , were drawn as four apparent resistivity maps to give spatial variation of apparent resistivity at penetration depths $AB/2 = 10, 100, 200$, and 400 m (Fig. 6a to 6d).

4. The best fit final models, one dimensional 1D, obtained from the inversion techniques is horizontally interpolated, taking into account the elevations of the sounding sites, to create six, two dimensional 2D, resistivity cross sections (Fig.7a-f). Along each of resistivity cross-section, the distinctive variations between the resistivity zones were marked as dashed lines.

5. Combining the resistivity cross-sections with the geological information and the geoelectrical calibration model (Table 1), six geoelectrical cross sections were constructed (Fig.8a-f).

Table 2. Interpretation results of the VES measurements by using IPI2win program.

profile VES No.	Resistivity (Ohm.m)							Thicknesses(m)					
	ρ_1	ρ_2	ρ_3	ρ_4	ρ_5	ρ_6	ρ_7	T1	T2	T3	T4	T5	T6
A-A'	16	11	21	6.2	52.4	11	63.4	1.36	13.1	7.4	35	125	
	36	0.9	4.23	86.4	11.9	913		0.42	13.4	19.1	310		
	35	3.66	10.4	70.1	5.01	23.1	20	1.59	15.1	8.96	47.4	103	
	23	136	2.92	22.4	1.95	87.5	3.71	1.98	2.34	9.17	13.4	60.5	
	25	23	12.6	4.2	25.4	4.29	>900	0.5	20.4	14.9	47.4	99.8	
	26	32.3	273	10.4	32	12	442	1.71	2.35	6.09	200	191	
	27	41.3	3.03	9.01	23.1	31.6		1.63	1.29	26.8	136		
	29	19.8	4.14	63.5	3.05	88.4	1.8	0.75	4.35	7.33	25.1	50.7	
B-B'	30	45.3	7.94	67.9	7.64	57.3	14.7	47	0.52	7.67	5.13	13.8	28.8
	17	59	13.5	121	9.88	89	102	0.95	1.43	5.47	8.6	223	
	22	10	5.6	30.7	3.8	56.9	6.6	88	1	2.7	5.4	23	
	37	34	5.8	54	4.6	90	7.6	38	2	1.7	3.2	7.2	
	24	>90	28.7	8.6	20.6	24	34.6		0.14	3.2	1.8	34.5	
	38	13.3	4.2	15.3	28				0.8	5.3	28.5	56.5	
C-C'	31	11.3	2.2	326	3.4	90			0.5	8.5	15.4	114	
	28	63	177	38	14.3	34.4	83	31	2.3	2.2	17	24.4	
	29	19.8	4.14	63.5	3.05	88.4	1.8		0.75	4.35	7.33	25.1	
	38	13.3	4.2	15.3	28				0.8	5.3	28.5		
	32	42	22	6.85	36	15.8			1.8	34	21	43	
	33	33	23	82	11.5	115			3.1	28.9	22	334	
D-D'	34	25.5	6.3	16.8	7.7	70	55.6	83	0.5	0.6	6.6	7.5	
	21	32	75.7	5.85	102	12.2	37	161	1.2	1.7	3.8	17.7	
	20	12	171	4.4	33	53	27	255	1.5	1.5	3.1	53.5	
	36	0.9	4.23	86.4	11.9	913			0.42	13.4	19.1	310	
	16	10.9	20.8	7.85	52.4	11.1	64.4		1.36	11.5	9.32	33.7	
	17	59	13.5	121	9.88	89	102		0.95	1.43	5.47	8.6	
E-E'	18	47	13	59	97.6	188			1.13	0.69	24.4	213	
	19	540	19	265	32.6	90	104		0.3	0.71	1.13	2	
	1	11.4	64	9.75	296	19	240		0.55	0.5	2.75	3	
	3	11.5	5.2	42.3	4	357	48		3.5	2	8.4	7.8	
	9	8.7	16	23	66				7	36	128	37	
	14	5.2	16.8	4.2	1113	49.5	20.7	50.7	1.46	10.6	9.87	49	
F-F'	15	29	77.6	16.6	55.6				2.34	15.3	61.7	102	
	16	11	21	6.2	52.4	11	63.4		1.36	13.1	7.4	35	
	1	11.4	64	9.75	296	20.4	246		0.55	0.5	2.75	3	
	2	31.7	78.6	21.2	129				1.64	49.5	41		
	4	33.6	11.4	17	48	12	104		1.5	8.5	88	182	
	5	11.7	3.7	13.7	5	84.6			2.5	2.1	85.5	93.4	
	7	7.5	17.4	63.3	7.8	55.6	41.5		0.24	5.5	5.3	7.6	
	8	311	11	95	147	33	223		0.25	3.64	16	33.5	
	12	43.6	98.5	22	71	36	316	60	0.9	0.96	2	25.6	
	13	14.9	248	28.3	261	13.7	61	167	0.58	0.4	1.64	4.5	

Table 2. Continued

profile	VES No.	1 st aquifer (Alluvial)		2 nd aquifer (Volcanic)		3 rd aquifer (Sandstone)		Bed rocks		
		ρ	T	ρ	T	ρ	T	ρ	depth	
A-A'	16	6-21	22	11-53	160			>64	182	
	36	1-5	13.8	11-87	329			>900	343	
	35	3-11	16.7	5-70	159					
	23	2-136	26.9	3-88	Und.					
	25	4-23	35.8	4-26	147			>900	183	
	26	10-273	10.2	12-32	326			>90	336	
	27	3-41	29.7	23-32	136					
	29	4-64	37.5	2-88	Und.					
	30	7-68	27.1	13-57	Und.			--		
B-B'	17	9-121	16.45			89-102	223			
	22	3-30	32	6-60	104	88	Und.			
	37	4-54	14	7-90	Und.					
	24	8->90	40	24-35	Und.					
	38	4-15	34.6	28	Und.					
	31	2-11	9	4-326	129			>900	138	
C-C'	28	38-177	21.7	14-83	Und.					
	29	4-63	37.5	2-88	Und.					
	38	4-15	34.6	28	Und.					
	32	6-42	56.8	>15	Und.					
	33	23-33	32	12-82	356	115	Und.			
	34	6-25	15.2			55-70	206	>83	231	
D-D'	21	5-102	56	37	34.3			161	90.4	
	20	3-146	6.7							
	36	1-4	13.8	12-329	329			>900	343	
	16	8-21	21	14-40	187			>64	184	
	17	9-121	16.45			89-102	223			
	18	13-59	26.2			98	213	188	239	
	19	19-265	4			90-104	208	168	212	
E-E'	1	9-64	24					246	24	
	3	4-41	5.5	48-357	Und.					
	9	8-16	57	31.5	Und.					
	14	4-16	22	1113	44	97	71			
	15	29-77	17.6	16-55	Und.					
	16	6-21	22	11-53	160			>64	182	
F-F'	1	9-64	24					246	24	
	2	33.6	1.6	21-78	90			129	92	
	4	11-33	94	>28	Und.					
	5	5-13	90	>84	93	84.6	Und.			
	7	7-63	70							
	8	11-311	19.7	32-147	114			223	134	
	12	22-71	8	36-316	63.5	60.5	Und.			
	13	14-248	2.66	13-261	22	61	288	167	313	

Table 3. Chemical analysis data for the collected water samples from highly contamination areas (Abdulqader, 2005).

No.	Source	TDS Mg/l	pH	Cations							
				Na		K		Ca		Mg	
				epm	ppm	epm	ppm	epm	ppm	epm	ppm
1	pond	3583	9.2	55.12	1267	0.44	12	2.6	52	13.2	160
2	stream	3848	8.11	39.3	903	0.85	33	4.6	92	7	85
3	lagoon	4628	7.12	32.9	756	1.08	42	6.4	128	30.4	370
4	lagoon	2542	8.3	21.3	490	0.84	33	4	80	13.4	163
5	dam	1905	7.95	14.34	329	0.46	18	2.2	44	7	85
6	channel	2295	7.9	17.39	400	0.46	18	12	241	5.8	71
7	borehole	3466	6.5	21	482	0.36	14	7.4	148	24.4	297
8	Dug well	3263	7	16.51	380	0.38	15	15	301	18.2	221
9	borehole	2483	7.88	21.78	501	0.31	12	3	60	5.8	71
10	pond	1638	6.8	11.2	257	0.46	18	5.2	104	8.4	102
11	Dug well	1989	7	12.26	282	0.1	4	3.6	72	14.4	175
12	Dug well	1183	6.5	12.18	280	0.05	2	0.6	12	6	73

Table 3. Continued.

No.	Location	E	N	Anions							
				CL		HCO ₃		SO ₄			
				epm	ppm	epm	ppm	epm	ppm		
1	Ghee Factory	43 55 39.65	13 36 51.46	33.2	1177	31.4	1916	5.46	262		
2	Rasyan	43 55 06.34	13 37 29.62	32.8	1163	1.22	74	17.69	850		
3	Burayhi1	44 00 28.48	13 38 19.58	53.88	1910	7.2	439	9.02	433		
4	Burayhi2	43 59 49.01	13 39 31.61	18.8	666	2.66	162	16.81	807		
5	Amera	43 59 05.89	13 37 17.37	12	425	4.25	259	7.29	350		
6	Ussayfra	44 00 04.79	13 36 42.25	15.4	546	7.84	456	11.85	569		
7	Hawgalas8	43 59 48.17	13 36 52.50	32.24	1143	5.68	347	12.76	613		
8	Hawgala	43 59 49.67	13 36 55.45	26.66	945	2.02	123	18.19	874		
9	Hawban	44 04 26.98	13 36 15.27	17.36	615	4.1	250	8.16	392		
10	Asfang Factory	44 03 26.90	13 35 32.32	11.16	396	3.38	206	9.86	474		
11	AlJanad	44 06 45.20	13 37 48.59	17.98	637	4.32	264	14.46	695		
12	Burayhi	44 00 39.16	13 37 47.21	7.44	264	6.34	387	3.67	176		

Results and Discussion

The resistivity and thickness of the strata are directly related to type of lithology, structures and water content in the voids. Therefore, integration of the data can give valuable information on groundwater salinity or contamination. The following is a brief discussion of the attainable results.

Apparent Resistivity Maps

The preliminary interpretation of apparent resistivity maps (Fig.6a-d) shows that the apparent resistivity follows the topography and structural features. The resistivity patterns are almost parallel to the mountainous ranges with decreasing values towards the contaminated areas. The careful study of all prepared apparent resistivity maps shows the following remarks.

a) The maps in Fig.6a (for $AB/2 = 10$ m) indicates three low resistivity zones. The first zone is found in eastern part, extending from Al Hawban to Al Janad. The second zone is observed in Hidran area. The third is found in the downstream of Wadi Rasyan. These low resistivity zones (< 20 Ohm.m) are believed to be associated with shallow alluvial deposits containing salty water, or may be due to the wet fine top soil.

b) Figures (6b, c and d) represent the resistivity maps corresponding to higher exploration depths ($AB/2 = 100$ to $AB/2 = 400$ m). This map shows that the low resistivity zones became smaller, in Hawban, Hawgala, and Hidran areas, are still observed at greater exploration depth (to $AB/2 = 400$ m). While, in Al Janad and downstream of Wadi Rasyan, the low resistivity zones are not observed.

c) Linear trends of resistivity contours separating the different resistivity zones may indicate structural barriers such as faults, dykes and igneous intrusions. The trends of the low resistivity zones are observed along the N-S in Hawban area, and along the SW-NE in Hawgala - Hidran area that coincide with major fault planes.

d) From the quality classification of the groundwater we can conclude the following; 1) The salty and brackish water is concentrated in Hawban, and Hidran areas. In these areas the salty or contaminated zones may extend to greater than 150 m depth. 2) Mineralized groundwater appears to extend widely surrounding the central part of the

study area, and 3) Fresh groundwater is more localized in the upstream of the wadis in Hayma, Dabab, and Wadi Rahaba.

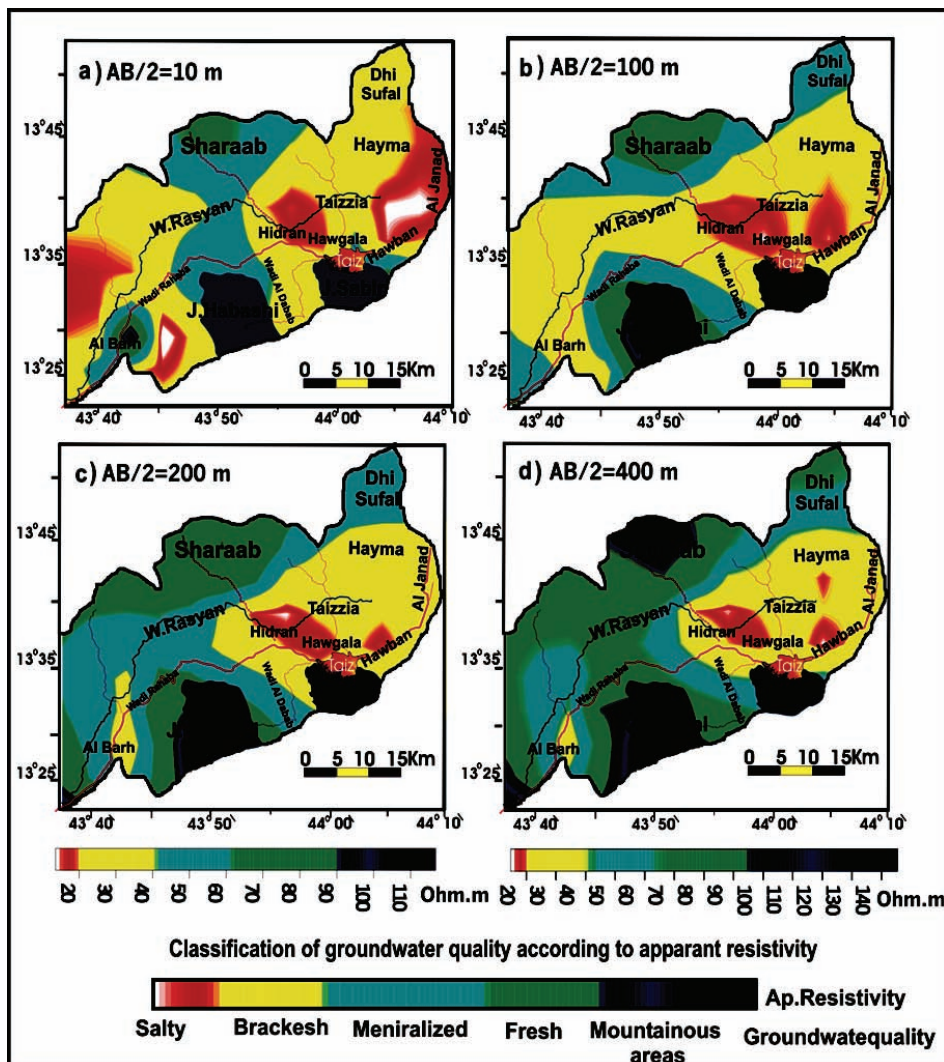


Fig. 6. Apparent resistivity maps of Uplands of Wadi Rasyan at different electrode distances; a) $AB/2 = 10\text{ m}$, b) $AB/2 = 100\text{ m}$, c) $AB/2 = 200\text{ m}$; and d) $AB/2 = 400\text{ m}$.

True Resistivity Cross-Sections

The distinctive variations in both lateral and vertical resistivities, were illustrated in form of true resistivity cross-sections shown in Fig. 7a to f. Above the ground surface line, the locations of sounding sites are shown, including the execution order numbers along the profiles. From

the interpretation of the resistivity cross-sections, it can be seen that there are many low resistivity regions (red color) in the sections where subsurface zones are far from a horizontal continuation. Along each profile, the different resistivity zones were marked with dashed lines.

The following is a brief discussion of true resistivity variations along the different profiles:

Along profile A-A' (Fig.7a), the low resistivity zone (<15 Ohm.m) is found below most of extensions from Hawban (VES-30) to Hidran (VES-36), it ranges in thickness between 10 and 50 m with the maximum thickness (50 m) below the VES-25 (Hawgala). This zone can be correlated with the surface alluvial deposits containing brackish water. At greater depth, the low-resistivity zone is observed below the VES-29 in (Hawban) and VES-23 (Wadi Al Malih) with the maximum thickness (329 m) below the VES-29 (Hawban). This zone may be considered as fracture basalts containing high dissolved salts (contaminated zones).

Profile B-B' (Fig.7b) shows presence of near surface low resistivity zone (< 10 Ohm.m) at the eastern side of the profile (Al Janad), this low resistivity zone may be due to fine or loose sediments of al Janad plateau. Another low resistivity zone is observed below the VES-22 (Akhdoor) which is represented as graben like structure containing brackish water. At greater depth, intermediate resistivity zone (10- 40) is observed to extend between VES-38 (Wadi Mawsata) to VES-37 (Wadi Al Malih), it ranges in thickness between 20 and 100 m. This zone can be correlated with the fracture volcanic containing brackish water (contamination zone).

Along profile C-C' (Fig.7c), there is a fairly low lateral variation in resistivity at shallow depth and distinct electrical variations at depths. The Low resistivity zone (< 10 Ohm.m) is found only below VES-29 in Hawban area. The intermediate resistivity zone (10-40 Ohm.m) was found between VES-33 and VES38 in Wadi Mawsata with maximum thickness of about 200 m. Abrupt change in the resistivities at the two ends of the profile may indicate the presence of graben structure in the middle part bounded by two horst structures at the ends.

Profile D-D' (Fig.7d) gives clear indication about the variation in topography of the area which increases in elevation from the middle to the sides, it also indicates the graben like structure in middle part of the

profile (Hidran area) where low resistivity zone (<15 Ohm.m) extends from the surface to depth of about 300 m.

Profile E-E' (Fig.7e) shows a fairly broad high resistivity zone (>50 Ohm.m). The low resistivity zone is observed at shallow depth in some areas along the main stream of Wadi Rasyan similar to that below the VES-16, 9 and 1, it is represented as seepage of brackish water from the stream into the alluvial deposits with maximum thickness of about 57 m at the VES-9.

In profile F-F' (Fig.7f), a deep low resistive zone (10-50 Ohm.m) is observed only below VES-4 and 5 (Wadi Al Rub) and flanked by two high resistive zones. As the profile is located away of pollution, the low resistivity zone may be considered as graben like structure filled with fine to clay sediments containing fresh water.

Geological Interpretation of the Resistivity Data

The interpreted results of resistivity data are accompanied with the well lithology and hydraulic characteristics to construct six geoelectrical cross-sections (Fig.8a-f).

Along each of geoelectric cross-section the depths to the main lithological units were identified, the possible structural boundaries such as faults, rock intrusions and basin topography were inferred also. The resistivity characteristics along the different profiles are quite similar, so they are discussed together. Four principal geoelectric layers can be distinguished and depicted from the ground surface down to the maximum depth of investigation as in the following:

1. The first geoelectric layer (top-most layer) is interpreted as alluvial deposits that cover most of wadi valleys. This layer has a wide range of resistivity (5 - 400 Ohm.m) and thickness (5 - 60 m) depending on the topography. In this layer, the very low resistivity zone (< 10 Ohm.m) is detected below water table, at most of the VES-stations along the profile A-A` (Fig.8a), VES-22 and 37 in profile B-B` (Fig.8b), VES-29 and 38 in the profile C-C` (Fig.8c), and VES-16 and 36 in the profile D-D` (Fig.8d). These zones were interpreted as contamination zones that spread over the wadi valleys and extend downward through the faults and features into the fracture volcanics.

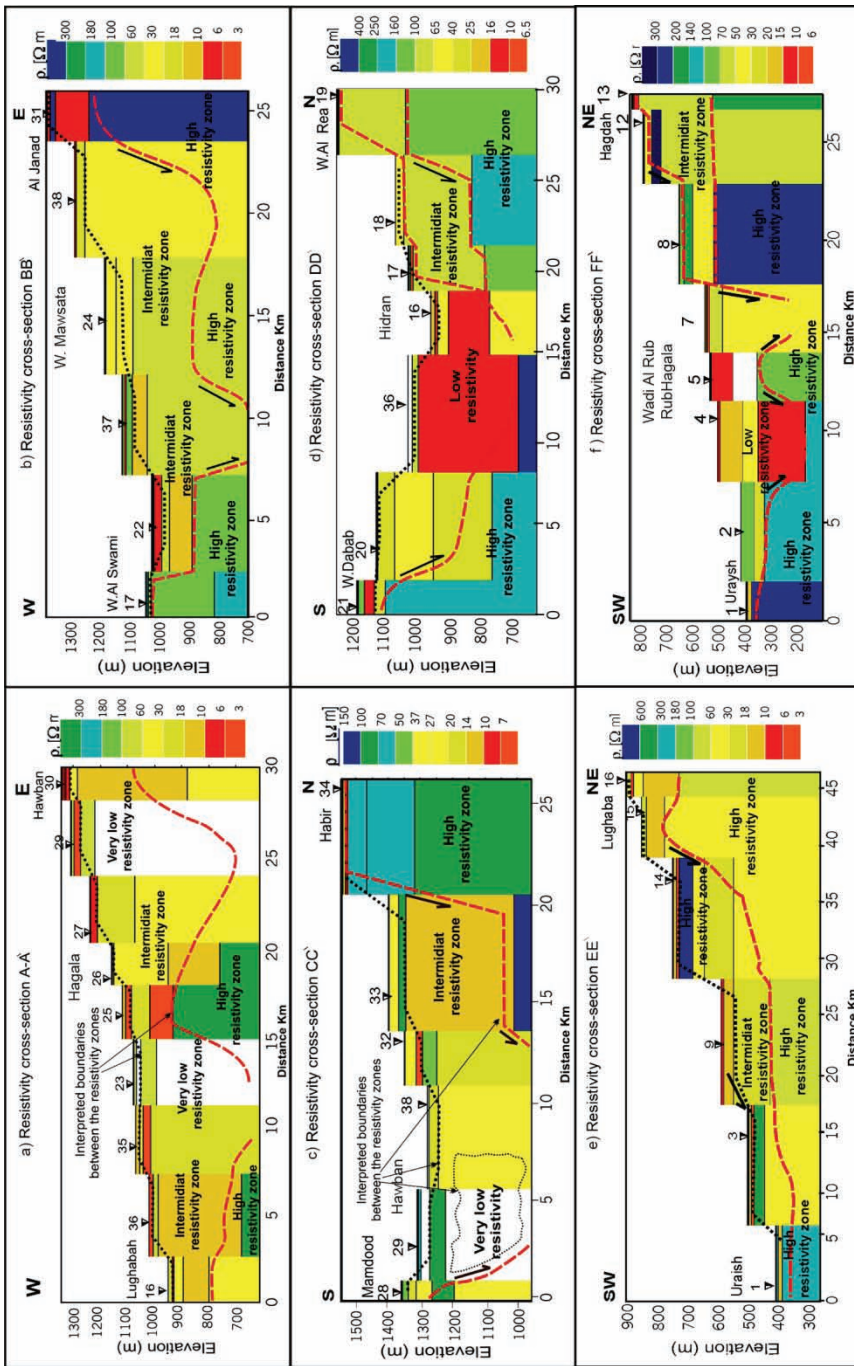


Fig. 7. True resistivity cross-sections obtained along the profiles A-A', B-B', C-C', D-D', E-E', and F-F'.

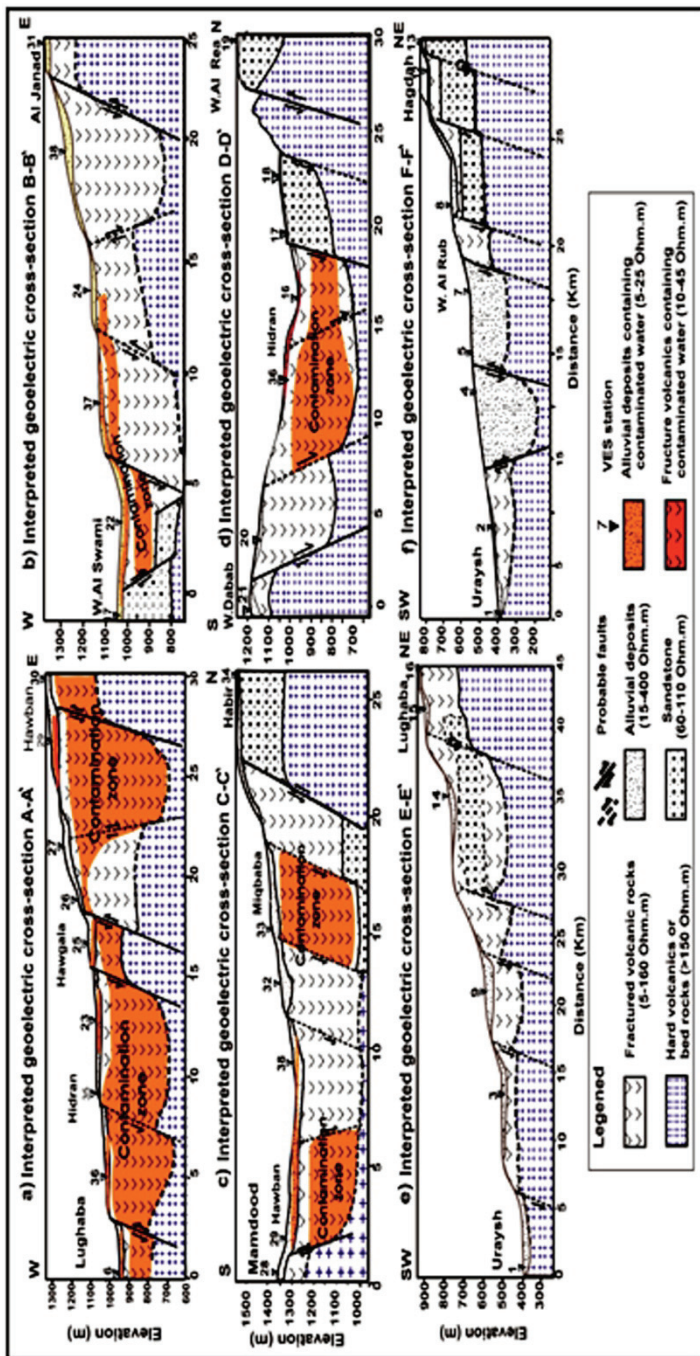


Fig. 8. Sub-surface geoelectrical cross-sections along the profiles, A-A', B-B', C-C', D-D', E-E', and F-F'.

2. The second geoelectric layer extends from the lower boundary of the near surface layer (alluvial deposits) in the valleys and plains, and from the surface in the hills and mountains. This layer is believed to be fracture volcanic rocks and can be divided into three zones.

a) The upper zone has resistivity greater than 50 Ohm.m is interpreted as dry weathered volcanic rocks or may be as dense volcanic layers in the bottom of the wadis. The thickness of this layer ranges between 9-60 m, its maximum thickness (60 m) is found below the VES-23 and its minimum thickness (9 m) is found below the VES-35 (Fig.7d).

b) The second zone is considered as wet or partly saturated fractured volcanic; it has resistivity ranges between 10 and 50 Ohm.m. Very low resistivity zones (<15 Ohm.m) were detected below most of the VES-stations in the profile A-A' (Fig.8a), below the VES-22, and 27 in the profile B-B' (Fig.8b), and below VES-29, and 33 in the profile C-C' (Fig.8c), below the VES-36, and 16 in the profile D-D' (Fig.7d). These zones concentrated in Taizia area where many contamination sources are found. The maximum thickness (300 m) of this zone is found below the VES-29 and the VES-35 in Wadi Al Hawban and Wadi Al Malih.

c) The third zone has resistivities greater than 100 Ohm.m. This zone is interpreted as hard acidic volcanics (rhyolite) or massif basalt which is forming a bed rock for the most of the study area (see Fig. 8a to f)

3. The third geoelectric unit has resistivity range between 70 and 110 Ohm.m. This geoelectric unit was interpreted as separated blocks of sandstone with thickness ranging between 70 to 288 m, it was detected as separated blocks closer to the surface at the northern ends of the profiles C-C' and D-D' (Fig. 8c and d). It was detected also at greater depth below VES-14 Wadi Rasyan (Fig.8e), and below VES-12 in Hagda, VES-8 in Wadi Al Rub (Fig.8f).

4. The deepest geoelectric layer is represented as bed rocks with resistivity (> 150 Ohm.m), it may be represented as hard basalt, rhyolite dyke complex, limestone or Precambrian basement.

Distributions of the Contamination Zones

The spatial extensions of the low resistivity zones have been outlined through interpretation of the apparent resistivity maps. Spatially,

three low resistivity zones have been identified. The frits, the largest one, extended from Hawgala to Lughaba passing through Wadi Al Malih and Hidran area, covering an area of about 15 Km². The second is found in Wadi Al Hawban covering an area of about 5 Km². The third is found along the main stream of Wadi Rasyan controlled by width of the valley.

The vertical extents of the low resistivity zones were identified through interpretation of the 2D resistivity sections. Along each of the 2D resistivity section, two resistivity zones were identified; 1) The shallow zone is observed in the alluvial deposits and along the stream of Wadi Rasyan, it extends to about 30 m depth and may extend down to the deeper layers. 2) The deep zone is detected in the volcanic layer with depths range between 70 and 300 m. In the vicinity of Taiz city (Hawban and Hidran areas), the very low resistivity zones were interpreted as possible leachate of contaminants from the disposal sites and sewage lagoons. In the other areas, low resistivity zones are considered as fine sediments or fracture volcanics containing high mineralized or hot water.

Pathways of Contaminants Transport

The contaminants follow both surface and subsurface pathways, surface pathways include the main stream of Wadi Rasyan stream, and ephemeral drainages passing through disposal sites. Type of rocks and intensity of fractures would play a major role in contaminant transport. The trend of the pollutant transport is observed along the N-S trend (Hawban-Al Janad) and along the SW-NE trend (Hawgala-Hidran area), coincide with the direction of groundwater flow.

The size of surface channels, how deeply they are filled, and the conditions of the subsurface geological discontinuity may all control the lateral and vertical distribution of the contaminant plumes. Therefore, the shallow subsurface contamination zones spread through the alluvial deposits of the wadis and along the stream of Wadi Rasyan. The deeper zone is spreading through the fissure and joints of fracture volcanics, along the major fault planes (NE-SW and NW-SE), and in the direction of groundwater flow.

Conclusion

The geoelectrical depth sounding provides useful information on groundwater pollution in the Uplands of Wadi Rasyans, Taiz, Yemen.

The seepage from sewage lagoons, industrial ponds, and disposal sites has produced serious deterioration of the groundwater resources. The contaminated or highly saline water has been found within both the surface alluvial and the deep fracture volcanic aquifers.

The low resistivity anomalies were detected in Taizzia area and along the main stream of Wadi Rasyan. Based on the geophysical, outcrop, and hydrochemical data, the low resistivity anomalies were interpreted as highly saline or contaminated zones, which are thicker (up to 140–150 m) in Hidran and Hawban areas, where many contamination sources are located.

The lateral resistivity inhomogeneities along the investigated profiles reveal development of graben like structure in the eastern part and step faulting in the western part of the study area.

The lateral and vertical spreading of the contamination zones are limited along the wadis and restricted by the mountains, they are generally oriented with directions of the major faults and consequently with the directions of groundwater flow.

References

- Ahmed Abdulqader.,** (2005) Geophysical and Hydrogeological studies for exploration and Evaluation of the Groundwater and its Environmental Protection in the Uplands of W.Rasyan, Taiz, Yemen. *Ph.D. Thesis, Assuit University, Egypt.*
- Barker, R.D.,** (1990) Improving the quality of resistivity sounding data in landfill studies. In: Ward, S.H. Ed., *Geotech. Environ. Geophys.* Vol. 1 Society of Exploration Geophysicists, pp: 245–251.
- Capaldi G., Chiesa S., Manetti P., and Piccardo G. B.,** (1983) Preliminary investigations on volcanism of the Sadah region (Yemen Arab Republic). *Bull. Volcanol.*, **46** (4): 413-427.
- Capaldi G., Chiesa S., Manetti P., Piccardo G. B., and Poli G.,** (1987a) Tertiary an organic granites of the western border of the Yemen Plateau. *Lithos.*, **20**: 433-444.
- Carpenter, P.J., Kaufmann, R.S., and Price, B.,** (1990) Use of resistivity soundings to determine landfill structure. *Ground Water* **28**: 569–575.
- Cartwright, K., and McComas, M.R.,** (1968) Surveys in the vicinity of sanitary landfills in northeastern Illinois. *Ground Water* **6**: 23–30.
- Chiesa, S., Civitta, L., De Fino, La Volpe, L., Lirer, L. and Orsi, G.,** (1989) The Yemen trap series: genesis and evolution of a continental flood basalt province. *J. Volcanol. Geotherm. Res.*, **36**: 337-350.
- Civitta L., La Volpe., and Lirer L.,** (1978) K-Ar age of Yemen plateau. *J. Volcanol. Geotherm. Res.*, **4**: 307-314.
- De Breuk, W. and De Moor, G.,** (1969) The water table aquifer in the eastern coastal area of Belgium. *Bull. Assoc. Sci. Hydro.* **14**: 137–155.
- DEY and UN/DDSMS,** (1997) Hydrological and land-use studies in Taiz region (Upper Wadi Rasyan Catchment) (TCD CONTRACT NO: YEM/93/010-3). Vol.1: *Main Report.* Dar El-Yemen Hydroconsultants DEY & SOAS.

- DHV Consulting Engineers.**, (1986) *Tihama Basin Water Resources Study Report*. Vol.1 and Vol.2, DHV, Amesfoort, the Netherlands.
- Edwards, L.S.**, (1977) A modified pseudosection for resistivity and IP: *Geophysics*, **42** (5): 1020-1036.
- Haeni, F.P., Lane, J.W., Jr., and Lieblich, D.A.**, (1993) Use of surface-geophysical and borehole-radar methods to detect fractures in crystalline rocks, Mirror Lake area, Grafton County, New Hampshire in Banks, D. and Banks, S., eds., *Hydrogeology of Hard Rocks*, Memoires of the XXIVth Congress, Oslo, Norway: *International Association of Hydrologists*, pp: 577-587.
- Goodell, H.G.**, (1986) A study of saltwater intrusion into the surface aquifer and the underlying of Yorktown Aquifer of Coastal Virginia. *Final Report to Virginia Environmental Endowment Richmond*, VA, 14p.
- Flanzenbaum, J.**, (1986) Evaluation of saltwater intrusion into the Coastal Aquifer of Southern Virginia. *M.Sc. Thesis*, Virginia Univ. press, 141p.
- IPI2win, Geoscan-M.**, (2001) A program for 1D automatic and manual interpretation of VES curves, Russia, Moscow, Moscow State University, Geological Faculty, *Department of Geophysics*.
- Klefsted, G., Sendlein, L.V., and Palmquist, R.C.**, (1975) Limitations of electrical resistivity methods in landfill investigations. *Ground Water* **13**: 418-437.
- Kruck W., and Schäffer U.**, (1991) Geological Map of Republic of Yemen (ROY). Scale 1:250,000 Taiz sheet. Ministry of Oil and Mineral Resources, Sana'a, Yemen, *Federal Institute of Geosciences and Natural Resources*, Hanover (FRG).
- Kruck W., Schäffer U., and Thiele J.**, (1996) Explanatory notes on the geological map of the Republic of Yemen- Western part. *Geologisches Jahrbuch*, Hannover.
- La Davison., Al Kadasi M., Al Khirbash S., Al Subbaray A. K., Baker J., Blkey S., Bosence D., Dart C., Heton R., McClay K., Menzies M., Nichols G., Owen L., and Yelland A.**, (1994) Geological evolution of the southern Red Sea Rift margin, Republic of Yemen. *Geol. Soc. America Bull.*, **106**: 1474-1493.
- Maxwell A. M.**, (2000) Geoelectrical investigation of old abandoned, covered landfill sites in urban areas: model development with a genetic diagnosis approach, *J. Applied Geophysics* **44**: 115-150.
- Meju, M.A.**, (1993) Geophysical mapping of polluted groundwater in a closed landfill site. In: 3rd Internat Congr. Brazil. *Geophys. Soc.*, Expanded Abstract. Pp: 425-428.
- Nowroozi, A.A., Stephen B. H. and Peter H.**, (1999) Saltwater intrusion into the freshwater aquifer in the eastern shore of Virginia: a reconnaissance electrical resistivity survey. *Applied Geophysics. J. Int.*, Vol. **42**, 1-22.
- RESIX-P, and Interpex**, (1993) Interpretation software with user's manual. Interpex, Golden, CO. USA.
- Stoller, R.L., and Roux, P.**, (1973) Earth resistivity survey: a method for defining groundwater contamination. *Ground Water* **13**: 145-150.
- Telford, W.M., Geldart, B.P. and Sheriff, R.E.**, (1976) *Applied Geophysics*, Cambridge University Press, London.
- Warner, D.L.**, (1969) Preliminary field studies using earth resistivity measurements for delineating the zone of contaminated groundwater. *Ground Water* **7**: 9-16.
- Welle J. van der.**, (1997) Hydrochemistry and pollution studies in the Upper Wadi Rasyan Catchment. *Unpublished Report*. 60 pp: plus appendixes.
- Whiteley, R.J., and Jewell, C.**, (1992) Geophysical techniques in contaminated lands assessment, *Explor. Geophys.* **23**: 557-565.
- Zohdy, A.A.R., Martin, P. and Bisdorf, R.J.**, (1993) A study of seawater intrusion using direct current soundings in the southeastern part of the Oxnard Plain, California. Open-File Report 93-524. *U.S. Geological Survey*, 139p.

استخدام طريقة الاستطلاع العمودي الكهربائي لاستقصاء نطاقات تلوث المياه الجوفية في مرتفعات وادي رسيان، تعز - اليمن

حمزة أحمد إبراهيم وأحمد سفيان الجابري * وأحمد عبد العزيز عبد القادر *

قسم الجيولوجيا - جامعة أسيوط،

* قسم الجيولوجيا - جامعة صنعاء،

** قسم الجيولوجيا - جامعة تعز

المستخلص. ازدادت الحاجة للمياه الجوفية وقل بالمقابل إمكانية الحصول على المياه العذبة منها، وذلك للزيادة المطردة في عدد السكان والتلوّن في النشاطات الزراعية، والصناعية، والمدنية، وإزداد الملوثات الناتجة عن تلك الأنشطة، وأثرت على المياه السطحية والجوفية، ولرصد ومتابعة تأثير الملوثات الذائبة في مياه الخزانات تحت سطحية تستخدم اليوم طريقة المسح الكهربائي السطحي والتي أصبحت من أكثر الطرق شيوعاً لسهولة تطبيقها وقلة تكلفتها. وبقياس المقامات الظاهرية وتحويلها لمقامات حقيقية يمكن رسم مقاطع جيوكهربائية توضح خصائص وأبعاد الطبقات تحت سطحية.

وفي هذه الدراسة استخدمت طريقة شلمبرجير لتوزيع الأقطاب وتم تنفيذ ٣٨ جسء كهربائي عمودية موزعة بطريقة مناسبة على ستة بروفيلات في أهم الوديان في منطقة مرتفعات وادي رسيان وذلك لمعرفة أبعاد نطاقات التلوث في خزانات المياه الجوفية، واستقصاء الظروف الجيولوجية تحت سطحية التي تحكم في اتجاه انتشار

نطاقات التلوك. وقد دلت نتائج تفسير تسجيلات المسح الجيوكهربائي على تأثر المناطق القريبة من المدينة بالملوثات المدنية والصناعية وتبين وجود:-

(١) أربع نطاقات تلوث قريبة من السطح ذات مقاومة منخفضة (أقل من ١٠ أوم) تظهر في مناطق الحوبان، الحوجلة، وحزان - وعلى امتداد وادي رسيان، و تميزت تلك النطاقات باتساعها (بين ٢ إلى ١٥ كم طول) ووصل سمكها إلى ٣٠ م وتنشر في رواسب الوديان السطحية. (٢) نطاقين عميقين اخترقا خزان رواسب الوديان في (وادي الحوبان) و(وادي الحوجلة- وادي المالح) إلى خزان البركانيات و إلى عمق أكثر من ١٥٠ م ، لكنهما أقل اتساعاً وقد أوضحت خرائط المقاومات الظاهرية على انتشار الملوثات في اتجاهات الفوالق والشقوق ومناطق التماس بين المكونات الصخرية المختلفة.

وأوصت الدراسة بإجراء مزيد من الدراسات الجيولوجية، الهيدرولوجية، وعمل نموذج لجريان المياه الجوفية في المنطقة، ومعرفة تأثير تراكيب المنطقة على انتشار نطاقات التلوك والعمل على بناء نظام متكامل لإدارة ومعالجة المخلفات المدنية والصناعية.